Brain Stimulation 15 (2022) 472–482

Contents lists available at ScienceDirect

Brain Stimulation

journal homepage: http://www.journals.elsevier.com/brain-stimulation

Cell type-specific excitability probed by optogenetic stimulation depends on the phase of the alpha oscillation

Mengsen Zhang [a], Flavio Frohlich [a, b, c, d, e, f, *]

[a] Department of Psychiatry, University of North Carolina, Chapel Hill, NC, USA
[b] Carolina Center for Neurostimulation, University of North Carolina, Chapel Hill, NC, USA
[c] Neuroscience Center, University of North Carolina, Chapel Hill, NC, USA
[d] Department of Cell Biology and Physiology, University of North Carolina, Chapel Hill, NC, USA
[e] Department of Biomedical Engineering, University of North Carolina, Chapel Hill, NC, USA
[f] Department of Neurology, University of North Carolina, Chapel Hill, NC, USA

ARTICLE INFO

Article history:
Received 8 November 2021
Received in revised form
30 January 2022
Accepted 21 February 2022
Available online 25 February 2022

Keywords:
Alpha oscillations
Optogenetics
Phase
Excitability
Gating
Synchronization

ABSTRACT

Background: Alpha oscillations have been proposed to provide phasic inhibition in the brain. Yet, pinging alpha oscillations with transcranial magnetic stimulation (TMS) to examine phase-dependent network excitability has resulted in conflicting findings. At the cellular level, such gating by the alpha oscillation remains poorly understood.

Objective: We examine how the excitability of pyramidal cells and presumed fast-spiking inhibitory interneurons depends on the phase of the alpha oscillation.

Methods: Optogenetic stimulation pulses were administered at random phases of the alpha oscillation in the posterior parietal cortex (PPC) of two adult ferrets that expressed channelrhodopsin in pyramidal cells. Post-stimulation firing probability was calculated as a function of the stimulation phase of the alpha oscillation for both verum and sham stimulation.

Results: The excitability of pyramidal cells depended on the alpha phase, in anticorrelation with their intrinsic phase preference; pyramidal cells were more responsive to optogenetic stimulation at the alpha phase with intrinsically low firing rates. In contrast, presumed fast-spiking inhibitory interneurons did not show such a phase dependency despite their stronger intrinsic phase preference.

Conclusions: Alpha oscillations gate input to PPC in a phase-dependent manner such that low intrinsic activity was associated with higher responsiveness to input. This finding supports a model of cortical oscillation, in which internal processing and communication are limited to the depolarized half-cycle, whereas the other half-cycle serves as a signal detector for unexpected input. The functional role of different parts of the alpha cycle may vary across the cortex depending on local neuronal firing properties.

1. Introduction

Brain stimulation is a key tool for the causal manipulation of neuronal networks in basic and clinical neuroscience. In particular, transcranial magnetic stimulation (TMS) [1] is widely used to non-invasively probe cortical excitability in humans [2–7]. One central question investigated with TMS is how cortical excitability is modulated by the alpha oscillation, which is thought to serve an inhibitory gating function of sensory processing [8–10]. Indeed, TMS-evoked responses have been reported to depend on alpha phase and/or amplitude [11–16]. Yet, given the number of confounding variables [17–19], the neuronal basis of such phasic gating of stimulation pulses remains poorly understood. To address this gap, we used optogenetic stimulation and single-unit extracellular recordings to directly investigate if and how exogenous input is rhythmically gated in the posterior parietal cortex, which generates alpha oscillations [20,21].

Alpha oscillations are the first recorded brain rhythm in human scalp electroencephalography (EEG) [22], initially observed at parietal-occipital locations at 8–12 Hz, most prominent when eyes were closed. Oscillations at a similar frequency range were later

* Corresponding author. Department of Psychiatry, University of North Carolina, Chapel Hill, NC, USA
E-mail address: flavio_frohlich@med.unc.edu (F. Frohlich).

https://doi.org/10.1016/j.brs.2022.02.014

found in various other cortical regions, such as the mu rhythm over central regions [23,24] and the tau rhythm over temporal regions [25]. Alpha-frequency rhythms observed at these distinct locations were thought to reflect a similar inhibitory process for the visual, somatosensory, and auditory systems respectively since they tend to diminish when the cortex is excited by stimuli (event-related desynchronization). Originally, alpha oscillations were considered to simply reflect an "idling" state [26]. However, more recent evidence suggests a more active role of alpha in information gating, such as suppressing irrelevant information or pulsed sampling [27–29]. At the level of the neurophysiological substrate, alpha oscillations are thought to realize the gating function by modulating cortical excitability over space and time [8–10]. In particular, part of the alpha cycle is considered the excitatory phase and another the inhibitory phase, corresponding to neuronal depolarization and hyperpolarization respectively. Delineating the role of alpha oscillations in modulating excitability is of translational importance since pathological changes in alpha oscillation have been implicated in various psychiatric [30–35] and neurological disorders [36,37].

TMS can be used as a tool to probe network excitability and thereby elucidate the role of oscillation phase on brain excitability in humans. Its application is most common in the primary motor cortex – a TMS pulse targeting a specific region can evoke involuntary contraction of the corresponding muscles, measured electrophysiologically as the Motor Evoked Potential (MEP) [1,2]. Analogously, stimulation of the visual cortex can evoke phosphenes (illusory flashing lights) [38,39]. The threshold and magnitude of evoked responses have been used as quantitative measures of cortical excitability. TMS-evoked MEP [16,40] or phosphenes [14,15] have been found to depend on the phase of the alpha oscillation, supporting the idea that alpha provides phasic inhibition to the respective brain regions. Though, the lack of such phase-dependency was also observed [41]. In addition to MEP or phosphenes-based methods most suitable for primary motor and visual cortices, TMS-evoked responses in EEG [42] and functional magnetic resonance imaging (fMRI) [43] were also found to depend on the alpha phase. Yet, EEG and fMRI responses are complex macroscopic outcomes of neuronal responses – the connection to neuronal excitability is indirect. Moreover, EEG-based results have not always been consistent with MEP-based results [44].

Inconsistency in the existing findings is in part due to the complex and non-specific nature of TMS-evoked response [45]. TMS is thought to primarily activate axons or white-matter tracts rather than cell bodies in the cortex [46,47]. Both pyramidal cells and inhibitory interneurons are subject to activation. Cortical responses also consist of multiple waves reflecting initial activation and subsequent polysynaptic network effects [48,49]. Moreover, within the body of work where alpha phase-dependency is observed, it remains unclear what exactly the more excitable phase in the alpha cycle is. Although negative peaks in surface EEG are sometimes assumed as the excitable phase [42] due to its association with the synchronized discharge of cortical pyramidal cells, actual observations based on evoked responses are rather diverse [14,15] or non-specific [16,40]. What is missing is a direct link between different phases of alpha to the underlying neuronal firing patterns and how this relationship impacts the response to stimulation.

The present study fills in this missing piece by using optogenetic stimulations targeted at random phases of alpha in the posterior parietal cortex (PPC) in ferrets. PPC is a key component of the posterior visual network, densely connected to the visual thalamus [50]. PPC exhibits strong alpha oscillation [21], thought to be a cortical driver of alpha oscillation in the visual network [20]. We show that the excitability of the pyramidal cells by stimulation is modulated by the alpha phase. In particular, they are more excitable at the less active alpha phase (low intrinsic firing rate). Our work highlights the crucial distinction and link between phase-dependent excitability and phase-dependent intrinsic activity.

2. Materials and Methods

2.1. Animals

Two adult spayed female ferrets (*Mustela putorius furo*, one year old at the beginning of the experiment) were used in this study. All animal procedures were performed in compliance with the National Institute of Health guide for the care and use of laboratory animals (NIH publication Np. 8023, revised 1987) and the United States Department of Agriculture and were approved by the Institutional Animal Care and Use Committee of the University of North Carolina at Chapel Hill.

2.2. Head-post, bone screws, virus injection, and optrode implantation surgery

The initial induction of anesthesia was performed with intramuscular injection of ketamine/xylazine (30 mg/kg of ketamine, 1–2 mg/kg of xylazine). After confirming the loss of paw pinch reflex, animals were intubated for isoflurane (0.5–2% in 100% oxygen) delivery via mechanical ventilation. The physiological parameters, including electrocardiogram, partial oxygen concentration, end-tidal CO2, and rectal temperature, were continuously monitored throughout the surgical procedure to maintain the animal in a stable state of deep anesthesia. All surgical procedures were performed under sterile conditions. The skull was fixed to a stereotactic frame using a mouthpiece and ear bars to enable accurate identification of target regions and electrode implantations. A custom-designed stainless-steel head-post was first secured to the anterior part of the exposed skull via four stainless steel bone screws. A craniotomy was performed over PPC of the left hemisphere to implant an optrode, i.e., a microelectrode array that includes an optical fiber (16 channel circular Platinum/Iridium electrode with a local reference electrode, 125 μm diameter, 5 mm length, 250 μm spacing; fiber optic 4.5 mm length, 200 μm core outer diameter; Microprobes for life science, Gaithersburg, MD). Before implantation, the dura and pia were removed; 0.4 μL of rAVV5-CaMKII-ChR2-mCherry was injected into PPC at three different depths (0.2 μL at 0.6 mm, 0.1 μL at 0.4 mm, 0.1 μL at 0.8 mm). The electrode tips were secured at the center of the virus injection site (13 mm AP, 3 mm ML, −0.6 mm DV relative to the occipital crest). Custom-designed plastic cylinders were implanted around the light fibers to anchor the optical fiber from the laser during recordings and to prevent laser light leakage. A bone screw close to the implant location on the left hemisphere was used as a ground for the optrodes. The optrodes were fixed in place with dental cement. After the dental cement hardened, the muscle and the skin around the incision were sutured together. Animals were administered preventative analgesics and antibiotics for one week after surgery while recovering in their home cage.

2.3. Optogenetic stimulation procedure and electric potential measurements

The ferrets were head-fixed and awake with eyes open during the stimulation and recordings. A blue laser at 475 nm (Shanghai Laser & Optics Century Co., Ltd., BL473T3) was used to activate the channelrhodopsin in PPC. Black sheets were applied as covers around the optic cable connection to avoid light leakage. Before each session, the laser power was calibrated to a specific level – 1,

2, 5, 10, 30 mW for Animal 1, and 1, 1.5, 2, 2.5, 3, 5, 10, 30 mW for Animal 2. Each session consists of 50–500 trials; each trial lasts 1s; inter-trial intervals were pseudo-random between 1 and 2s. In half of the trials in each session, laser pulses of 17 ms duration were administered in pseudo-random intervals to avoid forming a rhythmic structure. The pulse duration was chosen to provide sufficient time for ChR2 to reach plateau current at the lowest light intensity [51,52] and at the same time to be brief enough relative to an alpha cycle to provide sufficient phase resolution and to not substantially alter the macroscopic oscillation. The maximum number of pulses per trial was 10. No laser pulses were administered in the other half of the trials (sham). The order of stimulation and sham trials were randomly permuted within each session. The timing of the laser pulses and the trial design was controlled by a MATLAB program. Intracranial measurements of electric potentials were recorded simultaneously from the optrode in PPC for each session at a sampling frequency of 30 kHz. All stimulation and sham trials were visually inspected.

2.4. Verifying electrode position with histology

The animals were euthanized with an overdose of ketamine/xylazine after reaching the scientific endpoint and perfused immediately with 4% phosphate-buffered paraformaldehyde. After removing the brain from the skull, it was post-fixed overnight in the same solution, cryoprotected in 30% phosphate-buffered sucrose solution, shock frozen in dry ice, and cut into 50 μm thick sections with a cryostat (CM3050S, Leica Microsystems). Sections were stained for cells (Nissl). Imaging was conducted with an Aperio VERSA bright-field slide scanner at ×10 magnification. The electrode array was located in the sections by electrode tracks, tissue damage or loss, and by comparing and documenting the sections to ferret atlas plates [53].

2.5. Electrophysiological data analysis

Event-related potential, spectral analysis, and alpha phase-amplitude estimation. The raw electrophysiology data were low-pass filtered at 300 Hz and down-sampled to 1 kHz to obtain the local field potential (LFP). The LFP time series were visually inspected, and segments with high amplitude artifacts were rejected. The event-related potentials (ERP) or optogenetic-evoked potentials (OEP) were computed for each session as the LFP within an 80 ms window following the onset of each laser pulse averaged across all pulses. The power spectral density of the LFP was estimated using Welch's method (1s Hann window, no overlap). The peak alpha frequency of each animal was estimated between 10 and 20 Hz after removing the aperiodic (1/f-like) component from the spectra using FOOOF [54]. LFP in the channel with the highest peak alpha power was bandpass filtered for ± 3Hz around the animal-specific alpha frequency. Hilbert transform was used to estimate instantaneous alpha phase and amplitude from the bandpass filtered data. To accurately estimate the phase and amplitude of the ongoing alpha oscillation, ERPs were subtracted from LFP prior to bandpass filtering.

Spike extraction, sorting, and clustering. Kilosort2 [55], a toolbox based on a template matching algorithm, was used for initial spike extraction and sorting from raw electrophysiology data. Briefly, the raw data were high-pass filtered at 300 Hz, median-referenced, and whitened. Putative spike times were extracted from the pre-processed data based on threshold-crossing at −3.5 standard deviation below the average potential. These putative spike times were used to initialize a set of templates, i.e., putative spatiotemporal waveforms. Then, a matching pursuit algorithm was used to optimize the templates and infer spike times iteratively. As a final step for Kilosort, a heuristic algorithm was used to automatically merge certain templates based on the continuity of probability density distribution across the classification boundary. Following automated sorting in Kilosort, we performed an additional step of manual curation and template merging using Phy2 (https://github.com/cortex-lab/phy), producing the final single-unit (SU) assignment. The average waveform of each SU was computed using the raw data (broadband, 30 kHz). Subsequently, the waveforms were used to classify SUs into putative cell types – pyramidal cells (PYR) and fast-spiking inhibitory interneurons (INT). For each animal, Principal Component Analysis was applied to the time derivative of the waveforms to construct a two-dimensional feature space (first two principal components). The classification boundary was manually drawn between two clusters, and the resulting waveforms of each cluster were visually inspected to confirm putative cell identity.

Phase-locking value (PLV). The entrainment of spikes of each SU to the alpha oscillation was measured by PLV. The spike phase of the nth spike is defined as the instantaneous alpha phase θ at the spike time t_n. The PLV of a unit to the alpha oscillation is

$$PLV = \frac{1}{N}\left|\sum_{n=1}^{N} e^{i\,\theta(t_n)}\right|$$

, where N is the total number of spikes of the unit [56]. We used a fixed number of N = 200 randomly selected spikes per unit, computed PLV, and repeated 200 times for each unit. The mean PLV across all subsamples was the final result. The subsampling procedure was used to de-bias PLV from its dependency on N.

Null models of unit response to optogenetic stimulation. To assess unit response to optogenetic stimulation, we constructed null models that account for the intrinsic variability of unit activity and its dependency on the instantaneous alpha phase. To do so, we transported the laser pulse onset times in each stimulation trial to a randomly assigned sham trial for each session. We create 1000 different random reassignments of stimulation times for each session. Statistical measures (e.g., average firing rate change, firing probability density) based on the sham pulses were used to construct the mean and 95% confidence intervals of the null model.

Statistical analysis of the relation between neuronal excitability and intrinsic phase preference. We performed two types of analyses to measure the relation between excitability and intrinsic spike-phase dependency: (1) the correlation between excitability as a function of stimulation phase and intrinsic firing probability as a function of stimulation phase, and (2) the sum excitability at the preferred phase (i.e., where the intrinsic spiking probability density is greater than uniform distribution). More formally, phase-dependent excitability was defined as the difference between the post-stimulation firing probability density and post-sham firing probability (see Fig. 3a for illustration),

$$\Delta p_S[\theta_n] = p_S[\theta_n] - \frac{1}{M}\sum_{m=1}^{M} p^m_{null}[\theta_n]$$

where $p_S[\theta_n]$ is the post-stimulation firing probability density at the n-th phase bin θ_n (the alpha phase at stimulation onsets), $p^m_{null}[\theta_n]$ is the post-sham firing probability density at the n-th phase bin for the m-th random sample of sham windows, and M = 1000 is the total number of random samples of sham windows (see the construction of the null model above). $\frac{1}{M}\sum_{m=1}^{M} p^m_{null}[\theta_n]$ is the mean post-sham firing probability across all random samples, which is an estimate of the intrinsic firing probability density. To provide

sufficient phase resolution (i.e., sufficiently large number of phase bins) and to include a sufficient number of spikes for estimating firing probability (i.e., sufficiently large post-stimulation time window), we chose N = 12 as the number of phase bins and 10 ms as the duration of post-stimulation windows so that 1/12 of an alpha cycle is comparable to 10 ms.

The correlation (1) was defined as

$$r_{SI} = \frac{\sum_{n=1}^{N}(\Delta p_S[\theta_n] - \Delta\overline{p}_S[\theta_n])(p_I[\theta_n] - \overline{p}_I[\theta_n])}{\sqrt{\sum_{n=1}^{N}(\Delta p_S[\theta_n] - \Delta\overline{p}_S[\theta_n])^2}\sqrt{\sum_{n=1}^{N}(p_I[\theta_n] - \overline{p}_I[\theta_n])^2}}$$

where N is the number of phase bins, $\Delta p_S[\theta_n]$ is the excitability at the n-th phase bin θ_n, $\Delta\overline{p}_S[\theta_n] = \frac{1}{N}\sum_{n=1}^{N}\Delta p_S[\theta_n]$ is the average excitability, $p_I[\theta_n]$ is the intrinsic firing probability density at the n-th phase bin θ_n, and $\overline{p}_I[\theta_n]$ is the average intrinsic firing probability density over all phase bins. We also calculated the correlation coefficient r_{SI} for each sham sample by replacing $\Delta p_S[\theta_n]$ with $\Delta p^m_{null}[\theta_n] = p^m_{null}[\theta_n] - \frac{1}{M}\sum_{m=1}^{M} p^m_{null}[\theta_n]$ of the m-th random sample, which provided a null distribution of the correlation coefficients. For statistical analysis, the null distribution was used to provide the 95% and 99% confidence intervals to determine whether r_{SI} was significantly different from zero. We also reported the p-values for standard Pearson correlation analysis for reference.

The sum excitability at the preferred phase (2) was defined as

$$\Delta p_S^{pref} = \sum_{j=1}^{J}\Delta p_S\left[\theta_j^*\right]$$

where θ_j^* is the j-th phase bin where $p_I[\theta_j^*] \geq 1/(2\pi)$, i.e., where intrinsic firing probability density is above uniformity, and J is the total number of phase bins where intrinsic firing probability density was above uniformity. Like the correlation analysis above, the null distribution and confidence intervals were constructed using 1000 random samples of post-sham windows.

3. Results

12–17 Hz oscillations in the posterior parietal cortex (PPC) and the associated thalamocortical network in ferrets are considered the homolog of human alpha oscillations [20]. Electrophysiological activity in two awake, head-fixed ferrets was recorded to examine the relation between alpha oscillation and single-unit activity in the left PPC (Fig. 1a, Fig. 2a). Optogenetic stimulations were given at random intervals at the recorded site to probe the excitability of cortical neurons at different phases of alpha oscillation (Fig. 1b). We investigated three competing hypotheses: (1) stimulations increase neuronal firing rate independent of the alpha phase of the stimulation, i.e., neuronal excitability is phase neutral (Fig. 1c), (2) units preferentially increase firing rate when stimulations occur at their intrinsically preferred firing phase (red highlights in Fig. 1d), (3) neurons preferentially increase firing rate when stimulations occur outside of their intrinsically preferred firing phase (off red highlights in Fig. 1e).

An optrode was implanted at the left PPC (Fig. 2a–c) for simultaneous electrophysiology recording (Fig. 2d) and light stimulation of the channelrhodopsin. Both ferrets showed a prominent peak in the alpha frequency range (13.25 Hz for Animal 1, 13.28 Hz for Animal 2) in the frequency spectra (Fig. 2e). Individual-specific alpha peaks were used to bandpass-filter the LFP (Fig. 2d, bottom two traces) to estimate instantaneous alpha phase and amplitude for each ferret. Spikes were sorted into single units (SU), which were further classified into putative pyramidal cells (PYR) and putative interneurons (INT; Fig. 2f and g) based on their average waveform. The firing rate of each unit was computed for 10 ms before and after the onset of each laser pulse ("pre" and "post" in Fig. 2h and i). On average, the putative pyramidal cells of Animal 1 showed a significant increase in firing rate (t-test, $t(191) = 2.706$, $p = 0.007$). No significant firing rate changes were observed for Animal 1's interneurons ($t(43) = -0.453$, $p = 0.652$), or Animal 2's pyramidal cells ($t(181) = -0.111$, $p = 0.912$) and interneurons ($t(16) = 1.117$, $p = 0.281$). At the SU level, null models of pre- and post-stimulation firing rate were constructed for each unit using its activity in the sham trials. Units with firing rate change outside of the 95% CI were labeled in Fig. 2h and i (yellow, significant increase in firing rate; green, significant decrease in firing rate). For Animal 1, 20 units significantly increased firing rate (19 PYR, 1 INT), and 8 units significantly decreased firing rate (3 PYR, 5 INT). For Animal 2, 9 units significantly increased firing rate (8 PYR, 1 INT), and 6 units significantly decreased firing rate (6 PYR, 0 INT). Overall, these results indicate that few cells were highly responsive to light stimulation in terms of the average firing rate. For Animal 1, the population firing rate increase was dependent on laser power and most prominent for 10, 30 mW. We also observed a stimulation evoked potential (OEP) in Animal 1 (Fig. 2k), which was laser power-dependent (Fig. 2l). The OEPs were removed from the LFP before alpha phase estimation.

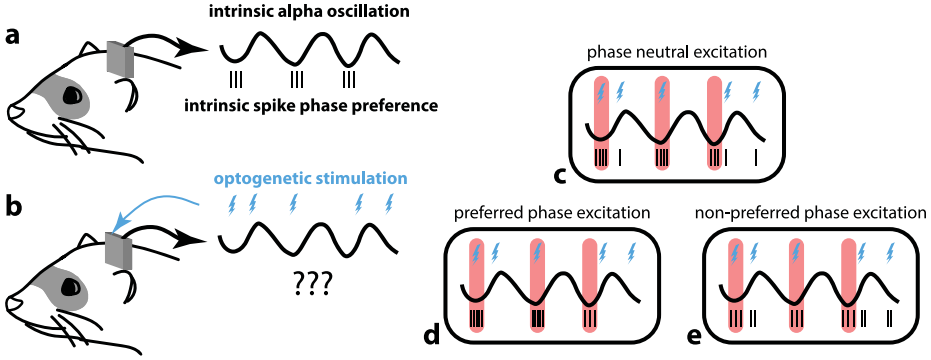

Fig. 1. Probing the modulating effect of the alpha oscillation on the excitability of cortical neurons. Neurons have different firing probabilities at different phases of the alpha oscillation (a). The left posterior parietal cortex (PPC) was stimulated with optogenetic tools at random phases of the alpha oscillation while neuronal spiking activities were measured (b). Three possible outcomes were considered: neurons are equally excitable regardless of whether the alpha phase is intrinsically preferred (highlighted in red) or not (c), neurons are more excitable at their intrinsically preferred phase (d), neurons are more excitable at their non-preferred phase (e). (For interpretation of the references to colour in this figure legend, the reader is referred to the Web version of this article.)

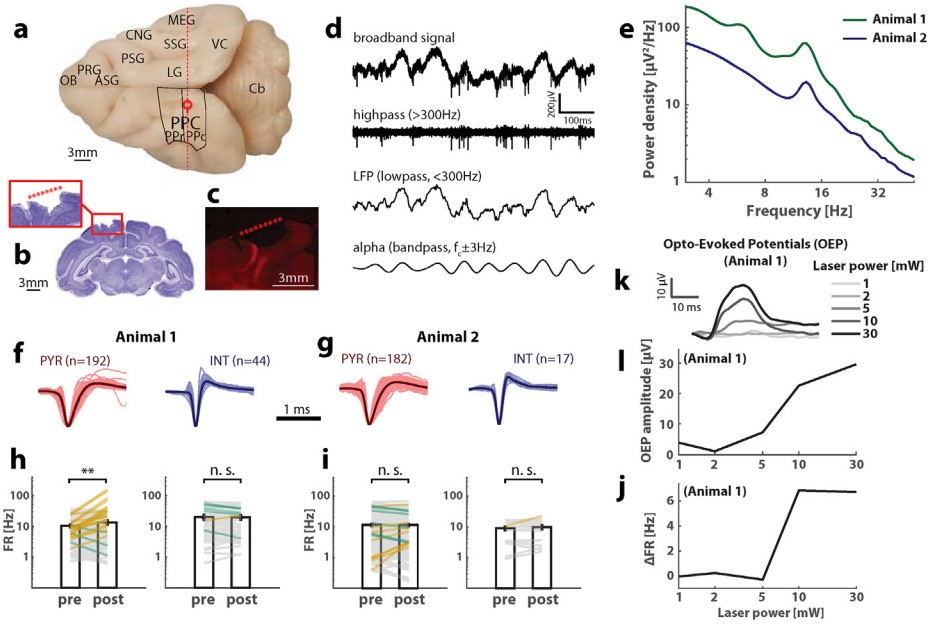

Fig. 2. Endogenous alpha oscillations and cell type-specific, power-dependent response to light stimulation. Optrode was implanted at the left posterior parietal cortex (PPC, with a caudal part PPc and a rostral part PPr) of the ferrets (red circle, a; lesions in b, c), following viral injection of CaMKII-ChR2-mCherry at the same location (florescent in c). Main cortical areas are labeled in (a): olfactory bulb (OB), proreal gyrus (PRG), anterior sigmoid gyrus (ASG), posterior sigmoid gyrus (PSG), coronal gyrus (CNG), lateral gyrus (LG), suprasylvain gyrus (SSG), medial ectosylvian gyrus (MEG), visual cortex (VC), and cerebellum (Cb). Spiking activity and alpha-frequency oscillations were conspicuous in the raw (broadband) signal (d, top). Unit activities were extracted from the high-pass filtered signal (2nd trace in d), and alpha phase and amplitude were estimated from the bandpass filtered signal around each ferret's peak alpha frequency (f_c; bottom trace in d). Both animals showed a prominent peak in the alpha frequency range (10–16 Hz) in the power spectra (e). Units were classified by the normalized spike waveforms (peak amplitude normalized to 1) into putative pyramidal cells (PYR) and interneurons (INT; f, g). Cell type-specific pre- and post-stimulation firing rates (FR) are shown in (h, i; mean ± SEM), where yellow lines highlight units that significantly increased firing rates, and green lines for those with significantly decreasing firing rates. Animal 1 showed clear laser power dependency of firing rate increase (ΔFR; j). In addition, optogenetic simulation-evoked potentials (OEP) were observed in LFP (k), with laser power-dependent amplitude (l). (**$p < 0.01$). (For interpretation of the references to colour in this figure legend, the reader is referred to the Web version of this article.)

Next, we examined the relation between spike timing and the phase of ongoing alpha oscillations. Without stimulation (sham condition), neuronal firing probability waxed and waned across different alpha phases (Fig. 3a.i for conceptual illustration, b.i and c.i for real data). Interneurons showed a stronger intrinsic phase preference than pyramidal cells (Fig. 3: blue curves in b.i and c.i further from uniformity than red curves), quantified as significantly greater phase-locking values (PLV) for interneurons than pyramidal cells in sham trials (d, e). The PLV in stimulation trials were not significantly different from the sham trials (paired t-tests: Animal 1, $t(191) = -1.25$, $p = 0.21$ for pyramidal cells, and $(t43) = 0.73$, $p = 0.47$ for interneurons; Animal 2, $t(181) = 0.69$, $p = 0.49$ for pyramidal cells, and $t(16) = -0.63$, $p = 0.54$ for interneurons). To understand neuronal excitability as a function of the alpha phase, we examined how the intrinsic firing probability was modified by light stimulations at different alpha phases. Specifically, we defined excitability as the difference (Fig. 3a.iii) between the post-stimulation firing probability (10 ms window, Fig. 3a.ii) and intrinsic firing probability (Fig. 3a.i). For the following analyses, we removed spikes that occurred at very low alpha amplitude (<10 μV), since in the absence of the alpha oscillation, the phase estimation would not be meaningful (see Fig. 4ab for the dependency of intrinsic spike phase on alpha amplitude). Including these low alpha amplitude spikes leads to qualitatively identical results. In both animals, the excitability of pyramidal cells (Fig. 3b.ii, c.ii) was anticorrelated with the phase preference (red, b.i, c.i), while the excitability of the interneurons (b.iii, c.iii) was not correlated with the phase preference (blue, b.i, c.i). For Animal 1, the Pearson correlation between the excitability and intrinsic phase preference of the pyramidal cells was $r = -0.723$, with $p = 0.0079$ (95% confidence interval, CI, of the null model is [−0.544,0.582]), and that of the interneurons was $r = 0.089$, with $p = 0.807$ (95% CI of the null model is [−0.692,0.707]). For Animal 2, the correlation coefficient for the pyramidal cells was $r = -0.707$, with $p = 0.010$ (95% CI of the null model is [−0.583,0.619]), and that of the interneurons was $r = -0.1425$, with $p = 0.659$ (95% CI of the null model is [−0.607, 0.603]). The phase dependency of excitability can also be measured by the sum excitability at the preferred phase: for Animal 1, the sum excitability at the preferred phase was −0.046 for pyramidal cells, significantly lower than zero (99% CI = [−0.028, 0.027]), and −0.017 for the interneurons, not significantly different from zero (95% CI = [−0.037, 0.037]); for Animal 2, the sum excitability at the preferred phase was −0.054 for pyramidal cells, significantly lower than zero (99% CI = [−0.040, 0.035]), and −0.034 for the interneurons, not significantly different from zero (95% CI = [−0.104,0.100]). These results are consistent with the correlation-based analysis above. The phase-dependent excitability in Animal 1 was extended to 30 ms after stimulation (sum excitability at the preferred phase was −0.0418, with 99% CI = [−0.022,0.020]; not significant for Animal 2 or interneurons, $p > 0.05$). Furthermore, in Animal 1, the anticorrelation for pyramidal cells depended on the laser power (Fig. 3f) in a similar fashion to that of the firing rate and optogenetic-evoked response (Fig. 2IJ). In short, pyramidal cells were found more excitable at the non-preferred phase, supporting the hypothesis in which the non-preferred phase exhibits the strongest response to stimulation (Fig. 1e).

Further, we investigated how neuronal spiking was influenced by the amplitude of alpha oscillations (Fig. 4). Given sufficient amplitude (>10 μV), neuronal spiking showed clear phase

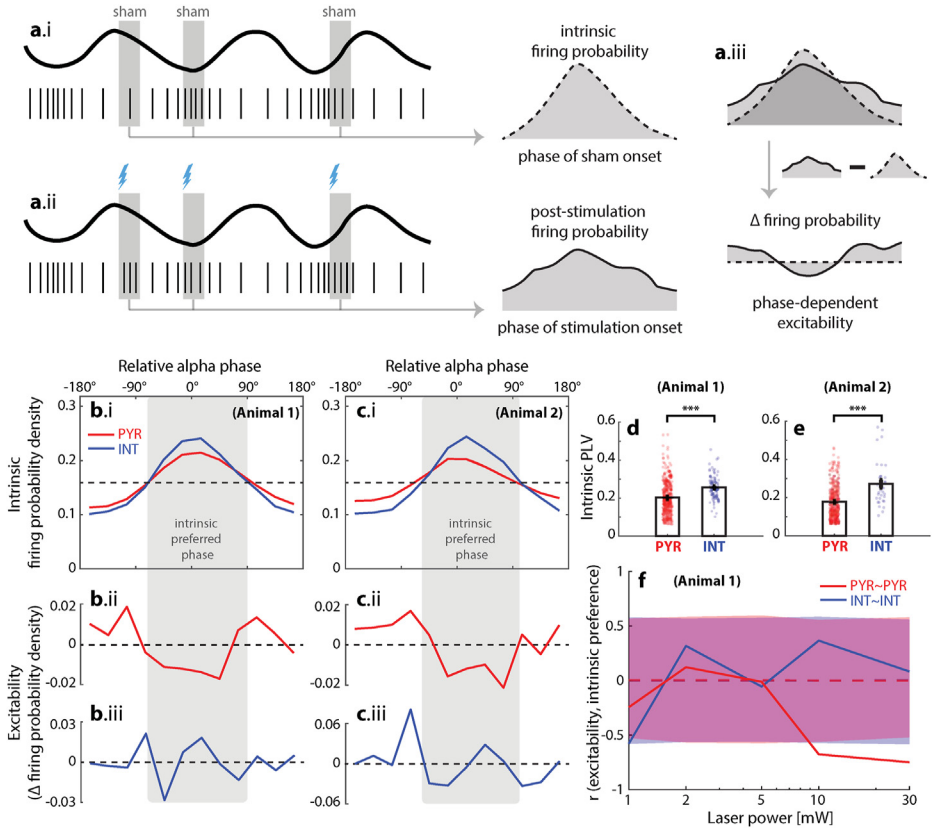

Fig. 3. Excitability anticorrelated with intrinsic alpha phase preference in pyramidal cells but not interneurons. (a) conceptually illustrates how to quantify unit excitability as a function of the alpha phase at the time of stimulation. Without stimulation, neuronal intrinsic firing probability as a function of the alpha phase was estimated in randomly sampled 10-ms windows (a.i). In stimulation trials, a similar firing probability function was calculated within 10-ms windows immediately following each stimulation onset (a.ii). The difference between the post-stimulation firing probability function and the intrinsic firing probability function (Δ firing probability) indicates the excitability of single units relative to their intrinsic activity at different alpha phases (a.iii). In the real data, single units of both animals showed strong phase preference (b.i, c.i), especially in putative interneurons (INT, blue) compared to pyramidal cells (PYR, red). Horizontal axes in (b, c) indicate the relative phase to the most preferred alpha phase of each animal (relative alpha phase = 0). The shaded area highlights where intrinsic firing probability density is greater than the uniform distribution. (d, e) shows a strong intrinsic phase preference of INT over PYR in terms of the phase-locking values (PLV) of spiking activity in the sham trials. PYRs had negative excitability at their preferred alpha phases in both animals (in b.ii, c.ii, red curves below dashed lines in shaded area) and positive excitability at their non-preferred phases (red curves above the dashed lines outside of shaded area). In Animal 1, the anticorrelation between the intrinsic phase preference and excitability of PYRs depended on laser power (f, red solid curve; red + purple area indicates the 95% confidence intervals of the corresponding null model). In contrast, INTs did not show such anticorrelation (solid blue curves in b.iii, c.iii, f; blue + purple area in f indicates the 95% confidence intervals of the corresponding null model). See text for detailed statistical results. (All error bars indicate standard errors. ***p < 0.001). (For interpretation of the references to colour in this figure legend, the reader is referred to the Web version of this article.)

dependency on alpha oscillations and such dependency increase with alpha amplitude (Fig. 4a and b). The intrinsic firing rates of pyramidal cells and interneurons were modulated by alpha amplitude in distinct manners (Fig. 4c and d; distributions estimated from 1000 random samples of post-sham windows, matched to the duration of post-stimulation windows as illustrated in Fig. 3a.i, a.ii). For pyramidal cells (PYR, Fig. 4c.i, d.i), higher alpha amplitude (greater than the median) was associated with lower firing rates (mean of distribution c.i is significantly lower than zero with $t(999) = -12.8$, $p < 10^{-34}$; mean of distribution d.i is significantly lower than zero with $t(999) = -27.9$, $p < 10^{-126}$). However, for interneurons (Fig. 4c.ii, d.ii), higher alpha amplitude was associated with higher firing rates (mean of distribution c.ii is significantly greater than zero with $t(999) = 13.6$, $p < 10^{-38}$; mean of the distribution d.ii is significantly greater than zero with $t(999) = 23.2$, $p < 10^{-95}$). The overall excitability of the neurons was not significantly modulated by alpha amplitude (Fig. 4e and f). For Animal 1, the excitability of pyramidal cells at the preferred phase was significantly lower for higher alpha amplitude (the difference between high and low alpha amplitude windows was −0.063, with 99% CI = [−0.053, 0.057]). This was not observed for Animal 2 or for interneurons. Overall, alpha amplitude-modulated intrinsic neuronal firing properties in a cell type-specific manner, but its effect on excitability requires further examination.

4. Discussion

In this study, we showed that the excitability of pyramidal cells in ferret PPC depended on the phase of the local alpha oscillation. Importantly, we connected the phase-dependency of neural excitability to the phase-dependency of intrinsic neuronal firing activity: excitability was anticorrelated with intrinsic phase preference (Fig. 3). These findings clarify the neurophysiological significance of alpha oscillations and provide clues about the functional role of different alpha phases that was elusive to noninvasive methods.

In the study of phase-dependent excitability, it is key to determine what is the more excitable phase. For scalp EEG, surface negativity has often been associated with synchronized depolarization of pyramidal cells [57], in particular for alpha oscillations [8,42,58] (note that the relation between surface negativity and firing rates can be reversed for other rhythms such as slow oscillations [59] and ultimately depends on the choice of reference). In the present study, we refer to this depolarization phase as the intrinsically preferred phase, or simply, the preferred phase (Fig. 1).

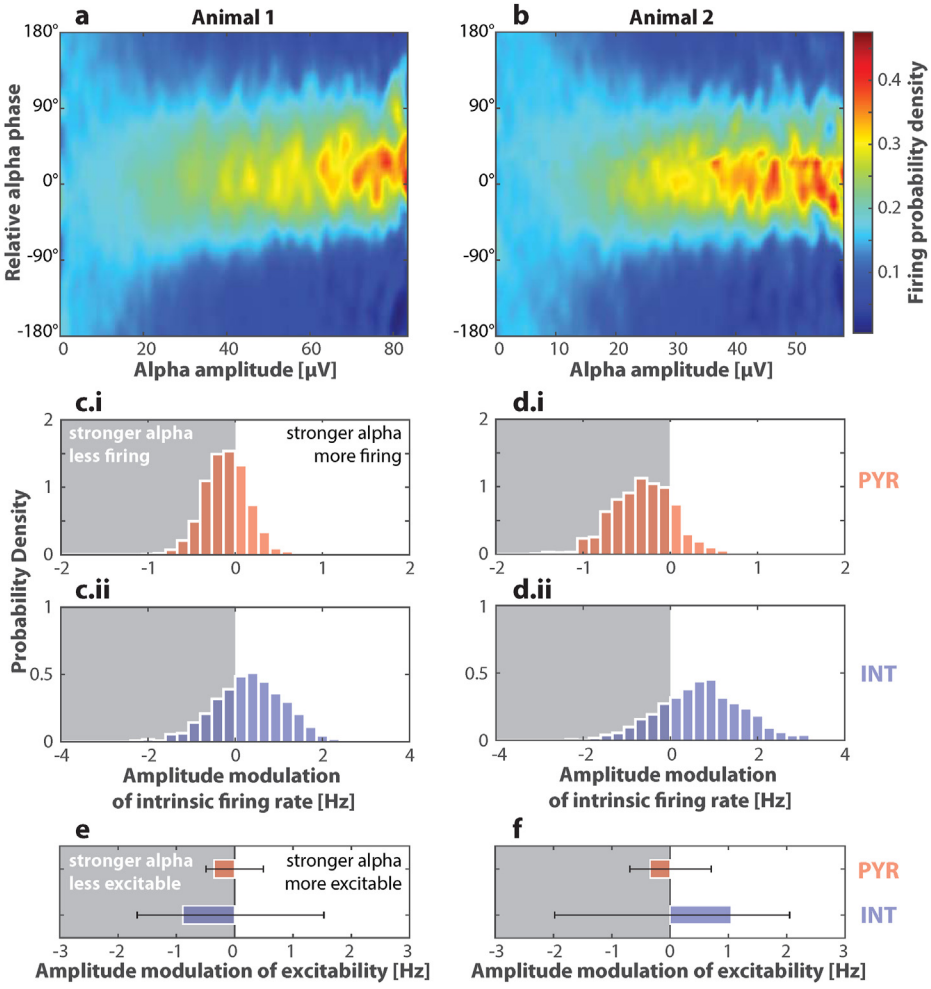

Fig. 4. Intrinsic neuronal spiking modulated by the amplitude of alpha oscillation. (a) and (b) show how alpha phase dependency of neuronal spikes (along the y-axis) was influenced by the amplitude of alpha oscillations (along the x-axis) for Animal 1 and 2, respectively. Y-axis indicates the spike alpha phase relative to the preferred phase (maximum firing probability over all amplitudes). Color indicates the conditional firing probability density of all single units over the alpha phase, given the alpha amplitude at the spike time. Neuronal spikes were more concentrated at the preferred phase when alpha amplitude was high. (c) and (d) show how intrinsic firing rates of pyramidal cells (PYR, c.i and d.i) and interneurons (INT, c.ii and d.ii) were modulated by alpha amplitude. The level of amplitude modulation (x-axes) was quantified as the difference between neuronal firing rates in sham trials with high alpha amplitude and those with low alpha amplitude (median split). The distributions were constructed using 1000 random sampling (see the construction of the null model in Materials and Methods). Negative modulation (shaded) means that higher alpha amplitude was associated with lower firing rates; Positive modulation (unshaded) means that higher alpha amplitude was associated with a higher firing rate. PYR (c.i, d.i) showed more negative modulation, while INT (c.ii, d.ii) showed more positive modulation. (e) and (f) show that the excitability of PYR and INT was not significantly modulated by alpha amplitude. Here the excitability was quantified as the difference between post-stimulation firing rate and intrinsic firing rate. Error bars indicate the 95% confidence intervals constructed from the null models. (For interpretation of the references to colour in this figure legend, the reader is referred to the Web version of this article.)

It is tempting to hypothesize (as we have, Fig. 1d) that the preferred phase is also the excitable phase – neurons may be more excitable when they are already depolarized. A similar position has been implied in existing works [42,60,61]. However, our results showed the opposite: the pyramidal cells were more excitable at the non-preferred phase (Fig. 1e; Fig. 3). In other words, our results suggest that neurons alternate between two functional phases in an alpha cycle: a depolarization phase, where intrinsic firing activity is high but responsiveness to additional input is low, and an excitable phase, where intrinsic firing activity is low but responsiveness to additional input is high. In the depolarization phase, multiple neurons in a network are firing in a small time window, which is thought to facilitate information integration and network communication [62]. In the excitable phase, the greater responsiveness to input, coupled with low intrinsic activity, is ideal for signal detection with a high signal-to-noise ratio [8]. Overall, our findings support a multifunction view of alpha oscillations (c.f. [63]), where half of the alpha cycle facilitates internal processing and communication while the other half facilitates signal detection.

What could be the cellular mechanism underlying this dissociation between the excitable phase and preferred phase? One plausible explanation is the sigmoidal shape of neuronal input-output response, i.e., how input currents are translated into firing rates (graphically as F–I curves; Fig. 5b,c). The derivative of an F–I curve indicates how the neuron would increase its firing rate given a small additional input, i.e., the excitability. F–I curves are typically sigmoidal, meaning the derivative (excitability) is small at both very low and at very high intrinsic firing rates (plateaus on the left end and right end in b,c), but large at intermediate intrinsic firing rates (steep increase in the middle of the curve). In other words, a neuron is most excitable at intermediate intrinsic firing rates. Now putting alpha oscillations back in the picture, if the firing rate at the preferred alpha phase (magenta asterisk in Fig. 5a) is in this intermediate range (magenta asterisk in b) and the firing rate at the non-preferred alpha phase (green asterisk in a) is in the low firing

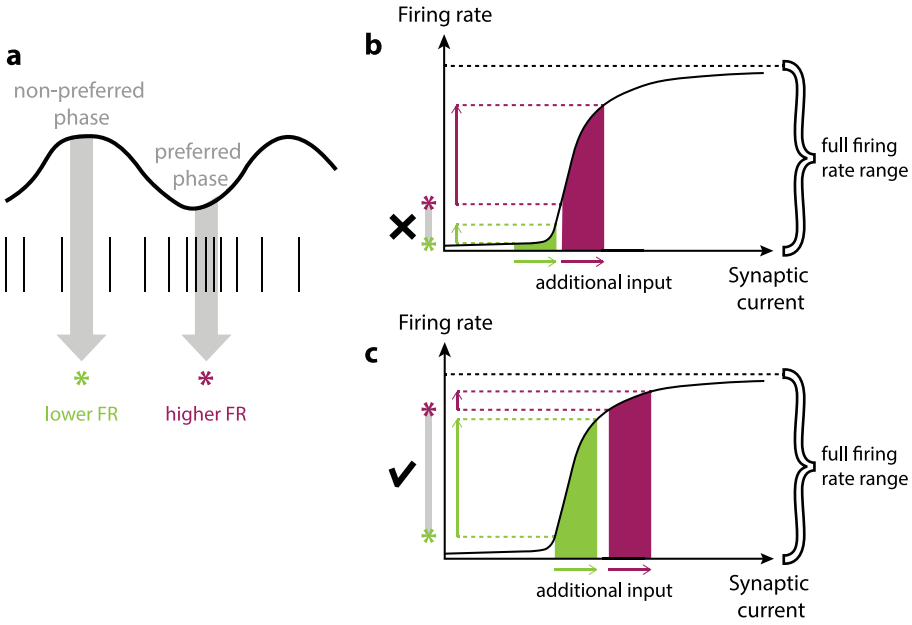

Fig. 5. Anticorrelation between intrinsic phase preference and excitability may be explained by features of the F–I curve. Without external stimulation, neuronal firing rates (FR) vary from low (green asterisk) to high (magenta asterisk) from the least preferred alpha phase to the most preferred alpha phase (a). Different firing rates reflect different levels of current input as often depicted by the F–I curve (b, c). If the alpha-regulated FR range (gray line connecting green and magenta asterisk in b) maps to the lower part of the full FR range (bracket), additional input at the preferred phase (magenta horizontal arrow) can induce a large FR increase (magenta vertical arrow), while input at the non-preferred phase (green horizontal arrow) can induce only a small increase in the FR (green vertical arrow) – opposite of the present experimental results. If the alpha-regulated FR range maps to a broad range (gray line connecting green and magenta asterisk in c), additional input at the preferred phase (magenta horizontal arrow) can lead to a small increase in FR (magenta vertical arrow) while the same amount of input at the non-preferred phase (green horizontal arrow) can lead to a large increase in FR (green vertical arrow) – consistent with the experimental results. (For interpretation of the references to colour in this figure legend, the reader is referred to the Web version of this article.)

rate range (green asterisk in b), the preferred phase would thus be more excitable than the non-preferred phase – this is the opposite of what we have observed. However, if the firing rate at the non-preferred phase is in the intermediate range (green asterisk in c) and the preferred phase is the high firing rate range (magenta asterisk in c), the non-preferred phase is more excitable – this is what we have observed in this experiment. Thus, which alpha phase is the more excitable phase depends not only on the phase itself, but also on where the alpha-regulated firing rate range (gray vertical line connecting the asterisks in b,c) is relative to the full firing rate range (large bracket). This explanation has two important implications: (1) knowing the alpha phase alone, without knowing the alpha-regulated firing rate range relative to the full firing rate range, is insufficient to predict what phase is more excitable, and (2) alpha oscillations may be considered as a more sophisticated gain control mechanism rather than a general inhibitory process.

The dependency of excitability on the firing rate range is likely to contribute to the variability of alpha oscillation's functional roles across cortical areas. Empirically reported excitable alpha phase varies from study to study and across regions [14,15,58,64]. Given that neuron firing properties vary across the cortex [65], it is possible that the same alpha phase does not have the same level of excitability and functional significance. Thus, the functional differentiation into internal processing versus signal detection phases suggested by our findings may be PPC-specific. Alpha oscillations in PPC are associated with high-level cognitive functions such as working memory [66,67] and attention [68,69] in suppressing task-irrelevant information to prioritize internal processing. Splitting an alpha cycle into internal processing and signal detection phases may help fine-tune the balance between top-down and bottom-up processing. However, primary sensory and motor cortices may demand less internal processing time than association cortices such as the PPC, while prioritizing the accurate gating of sensory input and motor output. Thus, in primary sensory and motor cortices, separating the alpha phase into internal processing and signal detection phase may be functionally inefficient. One could hypothesize that the excitable phase and the intrinsically preferred phase are more aligned in primary cortices. Additional experiments targeting pyramidal cells and interneurons in the sensory and motor cortices will elucidate the role of alpha oscillations in those regions and provide more comparable results to human TMS studies, where the visual [14,15] and motor cortices [40–42,44,60,70] were the primary targets. The interaction between alpha oscillation and neuronal firing rate range across the cortical hierarchy is worthy of further experimental examination.

Alpha phase dependencies observed in the present work differ by cell types (Fig. 3). Putative interneurons exhibited a stronger coupling to alpha oscillations, which is consistent with previous findings [21]. This may reflect a general contribution of interneurons to rhythm generation [71–73]. Phase-dependent excitability was only found in pyramidal cells but not interneurons, most likely due to the fact that channelrhodopsin expression was targeted to pyramidal cells – any effect on interneurons would have been indirect through the activation of pyramidal cells. The lack of second-hand phase-dependent excitability in interneurons suggests that the network interaction between the two cell types in response to stimulation is not straightforward.

Overall, our results support the idea that the phase of alpha oscillations modulates cortical excitability as observed in non-invasive human studies using TMS [14–16,40]. Nevertheless, the present study and human TMS studies differ in many aspects, including the mechanism of stimulation (optogenetics vs. TMS) and the mechanism of measurements (intracranial electrophysiology vs. MEP/phosphene/EEG). These distinctions lead to different

interpretations of excitability – primarily in terms of single-neuron excitability (the present study) vs. network excitability (TMS studies). The present optogenetic stimulation relies on the expression of light-activated cation channels in the membrane of pyramidal cells in a very confined region in PPC. Light stimulation opens the channels and permits transmembrane currents that induce subthreshold depolarization or trigger action potentials [74,75]. Thus, the evoked response mostly reflects single-neuron excitability in a manner similar to synaptic transmission. In contrast, TMS mainly induces currents along the white matter tracts, where the spatial derivative of the induced potential is high along the fiber [45]. As a result, excitability depends on the morphology of white matter fibers (bent fibers reduce the threshold of excitation). The response of stimulation may be at several nodes away from the site of activation [76], reflected as a multi-wave response structure in time, which was not observed in the present experiment. Thus, compared to the present optogenetic stimulation, TMS can induce network excitation in a more spatially and temporally extended and non-cell-type-specific manner. In parallel to the distinctions in stimulation mechanisms, single neuron response is accessible to highly localized intracranial electrophysiology but not to non-invasive measurements of excitability such as MEP, phosphene, or scalp EEG, while macroscopic and network effects do manifest at the motor, perceptual, and EEG level. In light of these mechanistic distinctions and existing findings in TMS studies, our findings suggest that alpha phase-dependent excitability observed in humans is at least in part due to the modulation effect of alpha oscillations on single neuron excitability.

Like all scientific studies, the present work has several limitations. First, while we have focused on immediate neuronal responses to stimulation in our analysis and theoretical explanation, network effects cannot be ruled out. To study the longer time scale network effects, an improved protocol with longer inter-stimulation intervals may be used. In the present study, few units have a significant firing rate increase (Fig. 2), and the overall firing rates have a small (Animal 1) to no (Animal 2) increase. This was intended as we wanted to probe neuronal excitability while minimizing network effects that would alter the macroscopic oscillation. A short post-stimulation window (10 ms) was chosen to provide sufficient phase resolution and specificity for our analyses of excitability within the alpha cycle (~75 ms). Light stimulation was administered a few times per second (roughly 1 stimulation per alpha cycle) in order to maximize the number of stimulations without altering the macroscopic oscillation. However, a single-pulse TMS stimulation protocol for humans typically involves seconds of inter-pulse intervals (IPI) [77,78], and stronger MEP has been observed for longer IPI [79]. Our short IPI protocol limits our ability to examine such long-term effects on cortical excitability. Thus, to reach conclusions more comparable to human TMS studies and to better examine the long-time scale network effects of brief simulation, an improved experimental protocol would be required with longer IPI at the time scale of seconds, and increased stimulation strength (higher laser power and opsin expression) to intentionally elicit stronger network effects. Second, optogenetic stimulation was only targeted at pyramidal cells. To fully understand the cell-type specificity in phase-dependent excitability, optogenetic stimulation of interneurons would be an important next step. Third, the experimental paradigm did not allow us to connect neuronal level excitability to cognition. Alpha-phase dependent perception have been observed in, e.g., visual perception [64,80,81], auditory perception [82] (c.f [58]. for tACS entrainment), and higher-level cognition [61,83]. Connecting target engagement by stimulation to performance in cognitive tasks would improve our understanding of the functional significance of phase-dependent excitability.

In conclusion, we found that neuronal excitability depended on the alpha oscillation in opposition to the intrinsic phase preference of neurons. It suggests that alpha oscillations in PPC alternate between an internal processing phase and a signal detection phase. We further provided a conceptual model of how the functional differentiation of alpha phases can result from the interaction between macroscopic oscillation and neuronal firing rate range. Together, our findings provide a window to the cellular-level mechanisms of phase-dependent excitability inaccessible in noninvasive approaches. Future work utilizing computational modeling and advanced optogenetic stimulation may deepen our understanding of the cell type-specific and network mechanisms of phase-dependent excitability.

CRediT authorship contribution statement

Mengsen Zhang: Methodology, Software, Validation, Formal analysis, Data curation, Writing – original draft, Visualization. **Flavio Frohlich:** Conceptualization, Methodology, Writing – review & editing, Supervision, Funding acquisition.

Declaration of competing interest

The authors declare the following financial interests/personal relationships which may be considered as potential competing interests:

F.F. is the lead inventor of IP filed on the topics of noninvasive brain stimulation by UNC. F.F. is the founder and CSO of Pulvinar Neuro LLC. He owns shares in Pulvinar Neuro. The company played no role in this research. FF has received honoraria from the following entities in the last twelve months: Sage Therapeutics, Academic Press, Insel Spital, and Strategic Innovation. M.Z. declares no competing interests.

Acknowledgments

The authors would like to thank Nick Randolph, Wei A. Huang, and Peyton Siekierski for their assistance in the data collection process of this study. This work is supported by the National Institute of Mental Health (R01-MH111889, R01-MH122477).

References

[1] Barker AT, Jalinous R, Freeston IL. Non-invasive magnetic stimulation of human motor cortex. Lancet 1985;325(8437):1106–7.
[2] Pascual-Leone A, Tormos JM, Keenan J, Tarazona F, Cañete C, Catalá MD. Study and modulation of human cortical excitability with transcranial magnetic stimulation. J Clin Neurophysiol 1998;15(4):333–43.
[3] Day BL, Dressler D, Noordhout AMd, Marsden CD, Nakashima K, Rothwell JC, et al. Electric and magnetic stimulation of human motor cortex: surface EMG and single motor unit responses. J Physiol (Camb) 1989;412(1):449–73.
[4] Boroojerdi B, Meister IG, Foltys H, Sparing R, Cohen LG, Töpper R. Visual and motor cortex excitability: a transcranial magnetic stimulation study. Clin Neurophysiol 2002;113(9):1501–4.
[5] Ziemann U, Tam A, Bütefisch C, Cohen LG. Dual modulating effects of amphetamine on neuronal excitability and stimulation-induced plasticity in human motor cortex. Clin Neurophysiol 2002;113(8):1308–15.
[6] Sparing R, Mottaghy FM, Ganis G, Thompson WL, Töpper R, Kosslyn SM, et al. Visual cortex excitability increases during visual mental imagery—a TMS study in healthy human subjects. Brain Res 2002;938(1–2):92–7.
[7] Rosanova M, Casarotto S, Pigorini A, Canali P, Casali AG, Massimini M. Combining transcranial magnetic stimulation with electroencephalography to study human cortical excitability and effective connectivity. Neuromethods 2011:435–57.
[8] Klimesch W, Sauseng P, Hanslmayr S. EEG alpha oscillations: the inhibition–timing hypothesis. Brain Res Rev 2007;53(1):63–88.
[9] Jensen O, Mazaheri A. Shaping functional architecture by oscillatory alpha activity: gating by inhibition. Front Hum Neurosci 2010;4:186.
[10] Mathewson KE, Lleras A, Beck DM, Fabiani M, Ro T, Gratton G. Pulsed out of awareness: EEG alpha oscillations represent a pulsed-inhibition of ongoing cortical processing. Front Psychol 2011;2:99.

[11] Romei V, Brodbeck V, Michel C, Amedi A, Pascual-Leone A, Thut G. Spontaneous fluctuations in posterior α-band EEG activity reflect variability in excitability of human visual areas. Cerebr Cortex 2008;18(9):2010–8.
[12] Zarkowski P, Shin CJ, Dang T, Russo J, Avery D. EEG and the variance of motor evoked potential amplitude. Clin EEG Neurosci 2006;37(3):247–51.
[13] Sauseng P, Klimesch W, Gerloff C, Hummel FC. Spontaneous locally restricted EEG alpha activity determines cortical excitability in the motor cortex. Neuropsychologia 2009;47(1):284–8.
[14] Samaha J, Gosseries O, Postle BR. Distinct oscillatory frequencies underlie excitability of human occipital and parietal cortex. J Neurosci 2017;37(11):2824–33.
[15] Dugué L, Marque P, VanRullen R. The phase of ongoing oscillations mediates the causal relation between brain excitation and visual perception. J Neurosci 2011;31(33):11889–93.
[16] Schilberg L, Ten Oever S, Schuhmann T, Sack AT. Phase and power modulations on the amplitude of TMS-induced motor evoked potentials. PLoS One 2021;16(9):e0255815.
[17] Nikouline V, Ruohonen J, Ilmoniemi RJ. The role of the coil click in TMS assessed with simultaneous EEG. Clin Neurophysiol 1999;110(8):1325–8.
[18] Premoli I, Bergmann TO, Fecchio M, Rosanova M, Biondi A, Belardinelli P, et al. The impact of GABAergic drugs on TMS-induced brain oscillations in human motor cortex. Neuroimage 2017;163:1–12.
[19] Conde V, Tomasevic L, Akopian I, Stanek K, Saturnino GB, Thielscher A, et al. The non-transcranial TMS-evoked potential is an inherent source of ambiguity in TMS-EEG studies. Neuroimage 2019;185:300–12.
[20] Stitt I, Zhou ZC, Radtke-Schuller S, Fröhlich F. Arousal dependent modulation of thalamo-cortical functional interaction. Nat Commun 2018;9(1):2455.
[21] Huang WA, Stitt IM, Negahbani E, Passey DJ, Ahn S, Davey M, et al. Transcranial alternating current stimulation entrains alpha oscillations by preferential phase synchronization of fast-spiking cortical neurons to stimulation waveform. Nat Commun 2021;12(1).
[22] Berger H. Über das Elektrenkephalogramm des Menschen. Archiv Für Psych Und Nervenkrankheiten 1929;87(1):527–70.
[23] Gastaut HJ, Bert J. EEG changes during cinematographic presentation (Moving picture activation of the EEG). Electroencephalogr Clin Neurophysiol 1954;6(3):433–44.
[24] Pfurtscheller G, Neuper C. Event-related synchronization of mu rhythm in the EEG over the cortical hand area in man. Neurosci Lett 1994;174(1):93–6.
[25] Hari R, Salmelin R, Mäkelä JP, Salenius S, Helle M. Magnetoencephalographic cortical rhythms. Int J Psychophysiol 1997;26(1–3):51–62.
[26] Pfurtscheller G, Stancák A, Neuper C. Event-related synchronization (ERS) in the alpha band — an electrophysiological correlate of cortical idling: a review. Int J Psychophysiol 1996;24(1–2):39–46.
[27] Jensen O, Bonnefond M, VanRullen R. An oscillatory mechanism for prioritizing salient unattended stimuli. Trends Cognit Sci 2012;16(4):200–6.
[28] Klimesch W. Alpha-band oscillations, attention, and controlled access to stored information. Trends Cognit Sci 2012;16(12):606–17.
[29] Hwang K, Ghuman AS, Manoach DS, Jones SR, Luna B. Cortical neurodynamics of inhibitory control. J Neurosci 2014;34(29):9551–61.
[30] Merrin EL, Floyd TC. Negative symptoms and EEG alpha activity in schizophrenic patients. Schizophr Res 1992;8(1):11–20.
[31] Sponheim SR, Clementz BA, Iacono WG, Beiser M. Clinical and biological concomitants of resting state EEG power abnormalities in schizophrenia. Biol Psychiatr 2000;48(11):1088–97.
[32] Henriques JB, Davidson RJ. Regional brain electrical asymmetries discriminate between previously depressed and healthy control subjects. J Abnorm Psychol 1990;99(1):22–31.
[33] Leuchter AF, Cook IA, Hunter AM, Cai C, Horvath S. Resting-state quantitative electroencephalography reveals increased neurophysiologic connectivity in depression. PLoS One 2012;7(2):e32508.
[34] Eidelman-Rothman M, Levy J, Feldman R. Alpha oscillations and their impairment in affective and post-traumatic stress disorders. Neurosci Biobehav Rev 2016;68:794–815.
[35] Keehn B, Westerfield M, Müller R-A, Townsend J. Autism, attention, and alpha oscillations: an electrophysiological study of attentional capture. Biol Psy Cognit Neurosci Neuroimag 2017;2(6):528–36.
[36] Bosboom JLW, Stoffers D, Stam CJ, van Dijk BW, Verbunt J, Berendse HW, et al. Resting state oscillatory brain dynamics in Parkinson's disease: an MEG study. Clin Neurophysiol 2006;117(11):2521–31.
[37] Montez T, Poil S-S, Jones BF, Manshanden I, Verbunt JPA, van Dijk BW, et al. Altered temporal correlations in parietal alpha and prefrontal theta oscillations in early-stage Alzheimer disease. Proc Natl Acad Sci Unit States Am 2009;106(5):1614–9.
[38] Kammer T, Puls K, Erb M, Grodd W. Transcranial magnetic stimulation in the visual system. II. Characterization of induced phosphenes and scotomas. Exp Brain Res 2005;160(1):129–40.
[39] Marzi CA, Mancini F, Savazzi S. Interhemispheric transfer of phosphenes generated by occipital versus parietal transcranial magnetic stimulation. Exp Brain Res 2009;192(3):431–41.
[40] Berger B, Minarik T, Liuzzi G, Hummel FC, Sauseng P. EEG oscillatory phase-dependent markers of corticospinal excitability in the resting brain. BioMed Res Int 2014;2014:936096.
[41] Madsen KH, Karabanov AN, Krohne LG, Safeldt MG, Tomasevic L, Siebner HR. No trace of phase: corticomotor excitability is not tuned by phase of pericentral mu-rhythm. Brain Stimul 2019;12(5):1261–70.
[42] Desideri D, Zrenner C, Ziemann U, Belardinelli P. Phase of sensorimotor μ-oscillation modulates cortical responses to transcranial magnetic stimulation of the human motor cortex. J Physiol (Camb) 2019;597(23):5671–86.
[43] George M, Saber G, McIntosh J, Doose J, Faller J, Lin Y, et al. Combined TMS-EEG-fMRI. The level of TMS-evoked activation in anterior cingulate cortex depends on timing of TMS delivery relative to frontal alpha phase. Brain Stimul 2019;12(2):580.
[44] Desideri D, Zrenner C, Gordon PC, Ziemann U, Belardinelli P. Nil effects of μ-rhythm phase-dependent burst-rTMS on cortical excitability in humans: a resting-state EEG and TMS-EEG study. PLoS One 2018;13(12):e0208747.
[45] Terao Y, Ugawa Y. Basic mechanisms of TMS. J Clin Neurophysiol 2002;19(4):322–43.
[46] Patton HD. The pyramidal tract: its excitation and functions. Handbook of Physiology, Section 1. Neurophysiology 1960:837–61.
[47] Klöppel S, Bäumer T, Kroeger J, Koch MA, Büchel C, Münchau A, et al. The cortical motor threshold reflects microstructural properties of cerebral white matter. Neuroimage 2008;40(4):1782–91.
[48] Day BL, Rothwell JC, Thompson PD, Dick JPR, Cowan JMA, Berardelli A, et al. Motor cortex stimulation in intact man. Brain 1987;110(5):1191–209.
[49] Ahn S, Fröhlich F. Pinging the brain with transcranial magnetic stimulation reveals cortical reactivity in time and space. Brain Stimul 2021;14(2):304–15.
[50] Manger PR, Masiello I, Innocenti GM. Areal organization of the posterior parietal cortex of the ferret (mustela putorius). Cerebr Cortex 2002;12(12):1280–97.
[51] Ishizuka T, Kakuda M, Araki R, Yawo H. Kinetic evaluation of photosensitivity in genetically engineered neurons expressing green algae light-gated channels. Neurosci Res 2006;54(2):85–94.
[52] Nikolic K, Grossman N, Grubb MS, Burrone J, Toumazou C, Degenaar P. Photocycles of channelrhodopsin-2. Photochem Photobiol 2009;85(1):400–11.
[53] Radtke-Schuller S. Cyto- and myeloarchitectural brain atlas of the ferret (Mustela putorius) in MRI aided stereotaxic coordinates. 1 ed. Cham: Springer; 2018.
[54] Donoghue T, Haller M, Peterson EJ, Varma P, Sebastian P, Gao R, et al. Parameterizing neural power spectra into periodic and aperiodic components. Nat Neurosci 2020;23:1655–65.
[55] Pachitariu M, Steinmetz N, Kadir S, Carandini M, Harris K. Fast and accurate spike sorting of high-channel count probes with KiloSort. In: Lee D, Sugiyama M, Luxburg U, Guyon I, Garnett R, editors. Advances in neural information processing systems, 29; 2016.
[56] Lachaux JP, Rodriguez E, Martinerie J, Varela FJ. Measuring phase synchrony in brain signals. Hum Brain Mapp 1999;8(4):194–208.
[57] Freeman WJ. Mass action in the nervous system. London: Academic Press; 1975.
[58] Neuling T, Rach S, Wagner S, Wolters CH, Herrmann CS. Good vibrations: oscillatory phase shapes perception. Neuroimage 2012;63(2):771–8.
[59] Contreras D, Steriade M. Cellular basis of EEG slow rhythms: a study of dynamic corticothalamic relationships. J Neurosci 1995;15(1):604–22.
[60] Zrenner C, Desideri D, Belardinelli P, Ziemann U. Real-time EEG-defined excitability states determine efficacy of TMS-induced plasticity in human motor cortex. Brain Stimul 2018;11(2):374–89.
[61] Samaha J, Bauer P, Cimaroli S, Postle BR. Top-down control of the phase of alpha-band oscillations as a mechanism for temporal prediction. Proc Natl Acad Sci Unit States Am 2015;112(27):8439–44.
[62] Womelsdorf T, Schoffelen J-M, Oostenveld R, Singer W, Desimone R, Engel AK, et al. Modulation of neuronal interactions through neuronal synchronization. Science 2007;316(5831):1609–12.
[63] Palva S, Palva JM. Functional roles of alpha-band phase synchronization in local and large-scale cortical networks. Front Psychol 2011;2:204.
[64] Mathewson KE, Gratton G, Fabiani M, Beck DM, Ro T. To see or not to see: prestimulus α phase predicts visual awareness. J Neurosci 2009;29(9):2725–32.
[65] Shinomoto S, Kim H, Shimokawa T, Matsuno N, Funahashi S, Shima K, et al. Relating neuronal firing patterns to functional differentiation of cerebral cortex. PLoS Comput Biol 2009;5(7):e1000433.
[66] Riddle J, Scimeca JM, Cellier D, Dhanani S, D'Esposito M. Causal evidence for a role of theta and alpha oscillations in the control of working memory. Curr Biol 2020;30(9):1748–54. e4.
[67] Sauseng P, Klimesch W, Heise KF, Gruber WR, Holz E, Karim AA, et al. Brain oscillatory substrates of visual short-term memory capacity. Curr Biol 2009;19(21):1846–52.
[68] Benedek M, Schickel RJ, Jauk E, Fink A, Neubauer AC. Alpha power increases in right parietal cortex reflects focused internal attention. Neuropsychologia 2014;56:393–400.
[69] Wöstmann M, Lim S-J, Obleser J. The human neural alpha response to speech is a proxy of attentional control. Cerebr Cortex 2017;27(6):3307–17.
[70] Schilberg L, Oever ST, Schuhmann T, Sack AT. Phase and power modulations on the amplitude of TMS-induced motor evoked potentials. PLoS One 2021;16(9):e0255815.
[71] Cobb SR, Buhl EH, Halasy K, Paulsen O, Somogyi P. Synchronization of neuronal activity in hippocampus by individual GABAergic interneurons. Nature 1995;378(6552):75–8.
[72] Whittington MA, Traub RD. Interneuron Diversity series: inhibitory interneurons and network oscillations in vitro. Trends Neurosci 2003;26(12):676–82.
[73] Buzsáki G. Rhythms of the brain. Oxford University Press; 2006.

[74] Boyden ES, Zhang F, Bamberg E, Nagel G, Deisseroth K. Millisecond-timescale, genetically targeted optical control of neural activity. Nat Neurosci 2005;8(9):1263–8.
[75] Nagel G, Szellas T, Huhn W, Kateriya S, Adeishvili N, Berthold P, et al. Channelrhodopsin-2, a directly light-gated cation-selective membrane channel. Proc Natl Acad Sci Unit States Am 2003;100(24):13940–5.
[76] Amassian VE, Stewart M, Quirk GJ, Rosenthal JL. Physiological basis of motor effects of a transient stimulus to cerebral cortex. Neurosurgery 1987;20(1):74–93.
[77] Hanakawa T, Mima T, Matsumoto R, Abe M, Inouchi M, Urayama S-i, et al. Stimulus–response profile during single-pulse transcranial magnetic stimulation to the primary motor cortex. Cerebr Cortex 2009;19(11):2605–15.
[78] Valero-Cabré A, Amengual JL, Stengel C, Pascual-Leone A, Coubard OA. Transcranial magnetic stimulation in basic and clinical neuroscience: a comprehensive review of fundamental principles and novel insights. Neurosci Biobehav Rev 2017;83:381–404.
[79] Vaseghi B, Zoghi M, Jaberzadeh S. Inter-pulse interval affects the size of single-pulse TMS-induced motor evoked potentials: a reliability study. Basic Clin Neurosci 2015;6(1):44–51.
[80] Valera FJ, Toro A, John ER, Schwartz EL. Perceptual framing and cortical alpha rhythm. Neuropsychologia 1981;19(5):675–86.
[81] Busch NA, Dubois J, VanRullen R. The phase of ongoing EEG oscillations predicts visual perception. J Neurosci 2009;29(24):7869–76.
[82] Kayser SJ, McNair SW, Kayser C. Prestimulus influences on auditory perception from sensory representations and decision processes. Proc Natl Acad Sci Unit States Am 2016;113(17):4842–7.
[83] Strauss A, Henry MJ, Scharinger M, Obleser J. Alpha phase determines successful lexical decision in noise. J Neurosci 2015;35(7):3256–62.